Room temperature photon number resolving detector at telecom wavelengths

Contents

Room temperature photon number resolving detector at telecom wavelengths

Enrico Pomarico, Bruno Sanguinetti, Rob Thew, Hugo Zbinden.

Group of Applied Physics, University of Geneva, 1211 Geneva, Switzerland.

enrico.pomarico@unige.ch

Abstract: Large dynamic range room temperature photon number resolving (PNR) detectors can be very useful for measuring very low light intensities and for analyzing multiphoton quantum states. In this paper we present a PNR detector based on the up-conversion (UC) of telecom signal into visible wavelength and on its detection by a thermoelectrically cooled multi-pixel silicon avalanche photodiodode (APD), also known as Silicon Photon Multiplier (SiPM). An efficiency of 4% is attained and the poissonian statistics of input coherent states is maintained up to approximately 20 simultaneous detections. The cross-talk effects on the detected signal are estimated in order to properly calibrate the detector. This scheme can be used at arbitrary wavelengths above the visible spectral window with appropriate up-conversion.

OCIS codes:

References and links

1. C. Simon, H. de Riedmatten, M. Afzelius, N. Sangouard, H. Zbinden, and N. Gisin. Quantum repeaters with photon pair sources and multimode memories. *Physical Review Letters*, 98(19):190503+, 2007.
2. S. Félix, N. Gisin, A. Stefanov, and H. Zbinden. Faint laser quantum key distribution: Eavesdropping exploiting multiphoton pulses. *Journal of Modern Optics*, 48(13):2009–2021, 2001.
3. Z. Walton, A. V. Sergienko, M. Atatüre, B. E. A. Saleh, and M. C. Teich. Performance of photon-pair quantum key distribution systems. *Journal of Modern Optics*, 48(14):2055–2063, 2001.
4. E. Knill, R. Laflamme, and G. J. Milburn. A scheme for efficient quantum computation with linear optics. *Nature*, 409(6816):46–52, January 2001.
5. M. Avenhaus, K. Laiho, M. V. Chekhova, and C. Silberhorn. Accessing higher order correlations in quantum optical states by time multiplexing. *Physical Review Letters*, 104(6):063602+, Feb 2010.
6. P. Sekatski, N. Brunner, C. Branciard, N. Gisin, and C. Simon. Towards quantum experiments with human eyes as detectors based on cloning via stimulated emission. *Physical Review Letters*, 103(11):113601+, Sep 2009.
7. M. Fujiwara and M. Sasaki. Photon-number-resolving detection at a telecommunications wavelength with a charge-integration photon detector. *Opt. Lett.*, 31(6):691–693, March 2006.
8. M. Fujiwara and M. Sasaki. Direct measurement of photon number statistics at telecom wavelengths using a charge integration photon detector. *Appl. Opt.*, 46(16):3069–3074, June 2007.
9. D. Fukuda, G. Fujii, A. Yoshizawa, H. Tsuchida, R. Damayanthi, H. Takahashi, S. Inoue, and M. Ohkubo. High speed photon number resolving detector withtitanium transition edge sensor. *Journal of Low Temperature Physics*, 151(1):100–105, April 2008.
10. D. Fukuda, G. Fujii, T. Numata, A. Yoshizawa, H. Tsuchida, H. Fujino, H. Ishii, T. Itatani, S. Inoue, and T. Zama. Photon number resolving detection with high speed and high quantum efficiency. *Metrologia*, 46(4):S288–S292, August 2009.
11. A. Divochiy, F. Marsili, D. Bitauld, A. Gaggero, R. Leoni, F. Mattioli, A. Korneev, V. Seleznev, N. Kaurova, O. Minaeva, G. Gol'tsman, K. G. Lagoudakis, M. Benkhaoul, F. Levy, and A. Fiore. Superconducting nanowire photon-number-resolving detector at telecommunication wavelengths. *Nature Photonics*, 2(5):302–306, April 2008.

12. X. Hu, T. Zhong, J. E. White, E. A. Dauler, F. Najafi, C. H. Herder, F. N. C. Wong, and K. K. Berggren. Fiber-coupled nanowire photon counter at 1550 nm with 24% system detection efficiency. *Opt. Lett.*, 34(23):3607–3609, December 2009.
13. Perkin Elmer. *High-Speed, Low light Analog APD Receiver Modules LLAM Series datasheet*.
14. B. E. Kardynal, Z. L. Yuan, and A. J. Shields. An avalanche-photodiode-based photon-number-resolving detector. *Nature Photonics*, 2(7):425–428, June 2008.
15. J. Řeháček, Z. Hradil, O. Haderka, J. Peřina, and M. Hamar. Multiple-photon resolving fiber-loop detector. *Physical Review A*, 67(6):061801+, Jun 2003.
16. G. Zambra, A. Andreoni, M. Bondani, M. Gramegna, M. Genovese, G. Brida, A. Rossi, and M. G. A. Paris. Experimental reconstruction of photon statistics without photon counting. *Physical Review Letters*, 95(6):063602+, Aug 2005.
17. D. Rosenberg, A. E. Lita, A. J. Miller, and S. W. Nam. Noise-free high-efficiency photon-number-resolving detectors. *Physical Review A*, 71(6):061803+, Jun 2005.
18. G. Wu, Y. Jian, E. Wu, and H. Zeng. Photon-number-resolving detection based on ingaas/inp avalanche photodiode in the sub-saturated mode. *Opt. Express*, 17(21):18782–18787, October 2009.
19. R. T. Thew, H. Zbinden, and N. Gisin. Tunable upconversion photon detector. *Applied Physics Letters*, 93(7):071104+, 2008.
20. P. Eraerds, M. Legré, A. Rochas, H. Zbinden, and N. Gisin. Sipm for fast photon-counting and multiphoton detection. *Opt. Express*, 15(22):14539–14549, October 2007.
21. M. Akiba, K. Tsujino, K. Sato, and M. Sasaki. Multipixel silicon avalanche photodiode with ultralow dark count rate at liquid nitrogen temperature. *Opt. Express*, 17(19):16885–16897, September 2009.
22. G. Temporão, S. Tanzilli, H. Zbinden, N. Gisin, T. Aellen, M. Giovannini, and J. Faist. Mid-infrared single-photon counting. *Opt. Lett.*, 31(8):1094–1096, April 2006.
23. R. V. Roussev, C. Langrock, J. R. Kurz, and M. M. Fejer. Periodically poled lithium niobate waveguide sum-frequency generatorfor efficient single-photon detection at communication wavelengths. *Opt. Lett.*, 29(13):1518–1520, July 2004.
24. R. T. Thew, S. Tanzilli, L. Krainer, S. C. Zeller, A. Rochas, I. Rech, S. Cova, H. Zbinden, and N. Gisin. Low jitter up-conversion detectors for telecom wavelength ghz qkd. *New Journal of Physics*, 8(3):32, March 2006.
25. A. Feito, J. S. Lundeen, H. Coldenstrodt-Ronge, J. Eisert, M. B. Plenio, and I. A. Walmsley. Measuring measurement: theory and practice. *New Journal of Physics*, 11(9):093038+, 2009.
26. I. Rech, A. Ingargiola, R. Spinelli, I. Labanca, S. Marangoni, M. Ghioni, and S. Cova. Optical crosstalk in single photon avalanche diode arrays: a new complete model. *Opt. Express*, 16(12):8381–8394, June 2008.
27. S. Vinogradov, T. Vinogradova, V. Shubin, D. Shushakov, and K. Sitarsky. Probability distribution and noise factor of solid state photomultiplier signals with with cross-talk and afterpulsing. volume N 25-111. IEEE Nuclear Science Symposium Conference Record, 2009.
28. Y. Mizumura, K. Kodani, J. Kushida, and K. Nishijima. Study of the basic characteristics of ppd (sipm) for the next generation of iacts. 31st ICRC, LODZ 2009.

1. Introduction

Estimating the number of photons in an optical pulse is desirable for the implementation and/or the optimization of a variety of applications. Several clinical or research activities deal with the analysis of fluorescent compounds for the identification and quantification of chemical reagents or biological molecules. For this task the measurement of the intensity of non repetitive optical pulses over a wide range of values can be improved by the use of photon number resolving detectors (PNR). Some technological and commercial applications, like optical time domain reflectometry (OTDR), can also gain in speed and sensitivity if fast and reliable photon counting is used. In the field of quantum information science, photon number resolution can improve the performance of quantum repeater [1] and of QKD protocols [2, 3], as well as allow linear optics quantum computation [4]. PNR detectors can also help in the investigation of the properties of multi-photon quantum states, by means of loss independent measurements of high order correlation functions [5] or with threshold detection conditions [6].

PNR detectors would be very useful for these applications, if they could estimate photon numbers in single shot measurements. Indeed, the photon number distributions can be reconstructed with just one single photon detector if a sample of identical photon pulses is available [15, 16]. Actually, even in this case, PNR detectors can make the applications faster, since they provide more information per pulse with respect to single photon detectors.

	CIPD [7, 8]	TES [9, 10]	PND [11, 12]	Lin APDs [13]	Non Sat APDs [14]	This work
Room Temperature				✓	✓	✓
High efficiency	✓	✓				
Fast repetition rates			✓	✓	✓	✓
Large dynamic range						✓

Table 1. Qualitative comparison between the main PNR detection approaches in the telecom regime. CIPD = charge integration photodiode; TES = transistor edge sensor; PND = parallel nanowire detector; Lin APDs = linear APDs; Non Sat APDs = Non saturated mode APDs. For large dynamic range we mean a range between 0 and thousands of input photons.

Depending on the specific task to be performed, different features are demanded for a PNR detector. Quantum information tasks require a very efficient and high photon number resolution, but not necessarily a large dynamic range. On the contrary, PNR detectors with limited efficiency can be used for biological or chemical applications and for the investigation of multiphoton quantum states, but a large dynamic range is highly desirable in this case.

Table 1 qualitatively compares the PNR detectors working at telecom wavelengths. The charge integration photodiodes (CIPD) [7, 8] and transistor edge sensors (TES) [17, 9, 10] are very efficient and have good photon number resolution. However, they need cryogenic apparata for cooling, so they are expensive and cannot work as plug-and-play systems. Moreover, they work at quite slow repetition rates. Superconducting parallel nanowires detectors [11, 12] provide faster responses, but require cryogenic apparata as well. Avalanche photodiodes (APDs) in a linear mode, even with a very low noise equivalent power (NEP) [13], have a high minimum detectable number of photons (of the order of 10^3), and APDs in non-saturated mode [14, 18], where weak avalanches are measured at an early stage of multiplication, have a limited efficiency and photon number resolution.

In this paper, we present a PNR detector that works at telecom wavelengths, at room temperature, with a high readout frequency and large dynamic range. This provides a practical detector well suited to measuring low intensities of light in a single shot fashion or studying multiphoton quantum states. It is based on the up-conversion (UC) of telecom photons into the visible regime and their detection by a multi-pixel APD detector, also known as Silicon Photon Multiplier (SiPM). The use of the UC as an interface for detecting a telecom signal at the visible wavelength is already known [19], but this time it is used to exploit the photon counting capability of the SiPM [20, 21]. Moreover, the UC process allows this approach to be adopted for a wide range of longer wavelengths [22]. In the following sections, we describe the detection scheme and data acquisition process. A characterization of the detector is carried out by measuring its efficiency and noise, before we discuss its photon number counting capability.

2. The up-conversion multi-pixel APD detector

2.1. Scheme of the detector

A diode laser at 1559 nm provides pulses of 1 ns-width that can be attenuated down to the single photon level, as shown in Figure 1. The telecom signal is mixed with a cw pump diode laser at 980 nm (JDS Uniphase) in a fiber wavelength division multiplexer (WDM). The maximum emitted pump power is approximately 300 mW. After the WDM, the telecom signal and the pump are injected into a periodically poled lithium niobate (PPLN) waveguide (HC Photonics), where the non linear UC of the signal takes place. The polarization of the input beams is con-

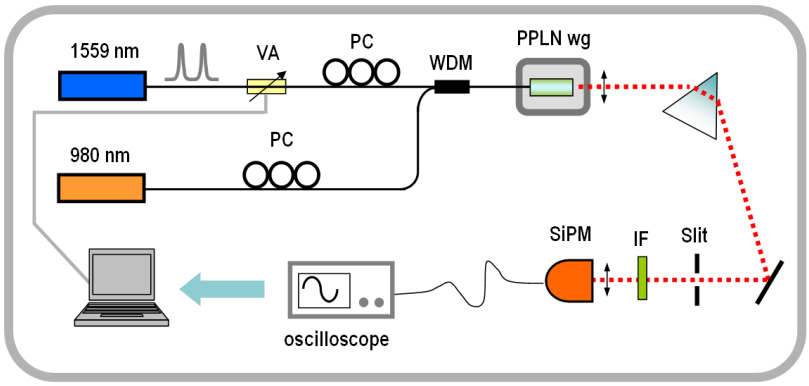

Fig. 1. Schematic of the up-conversion multi-pixel APD detector. Pulses from a diode laser at 1559 nm are attenuated (variable attenuator (VA) in the Figure) and injected, toghether with a pump laser at 980 nm, into a PPLN waveguide (PPLN wg), where the up-conversion takes place. Polarization controllers (PC) are used for optimizing the nonlinear process. Light at 600 nm is then filtered by a dispersion prism and an interference filter (IF), and detected by the SiPM. The electical signal is registered on the oscilloscope.

trolled to satisfy the quasi-phase matching (QPM) conditions. The waveguide has a length of 2.2 cm, a poling period of 9 μm, a nominal normalized internal efficiency of 500% W^{-1} cm^2 and its input is fiber pigtailed.

The condition for QPM is obtained at 76.6 °C and converts the signal at 1559 nm to 600 nm. The upconverted light is collimated and then filtered by a dispersion prism and an interference filter (IF) at (600±20) nm. In this way we remove the remaining pump photons and their second harmonic generation signal at 490 nm, at which the SiPM is quite efficient. The signal is then focused onto a free space SiPM (Hamamatsu Photonics S11028-100(X1)) with 100 APDs arranged on an active area of 1 mm^2 with a fill factor of 78.5%. The choice of the number of pixels is a compromise between the dynamic range, the efficiency and the photon number resolution of the detector. Indeed, a SiPM with more than 100 pixels would allow a wider dynamic range, but suffer from a lower photon sensitivity and efficiency. An internal Peltier cooler allows the detector to operate down to -34°C, corresponding to a breakdown voltage of 66.8 V. The electrical output is amplified with a 10 dB amplifier (Mini-Circuits, 0.1-500 MHz) and processed by a low-pass filter.

2.2. Data acquisition

Telecom wavelength optical pulses are sent to the detector with a 100 kHz repetition rate (see Figure 1). Their intensity can be set by varying the attenuation automatically by software. The signal detected by the SiPM is measured with a 500 MHz oscilloscope, triggered by a PIN photodiode that detects a portion of light from the optical source. The amplitude of the SiPM output, in a relatively low photon number regime, is approximately proportional to the number of simultaneous avalanches in the detector [20, 21]. In Figure 2 the superposition of the waveforms of the detected signal on the oscilloscope is shown. Their amplitudes take quite distinct values that are distributed according to the poissonian distribution of the number of detected photons. Their duration is approximately 50 ns.

For each coherent state sent to the detector, we register 10^5 traces from the oscilloscope and measure the height of the signal for each trace. The upper part of Figure 3 shows the pulse height histograms for coherent states with mean number of simultaneous detections $\langle n \rangle_{det}$ of

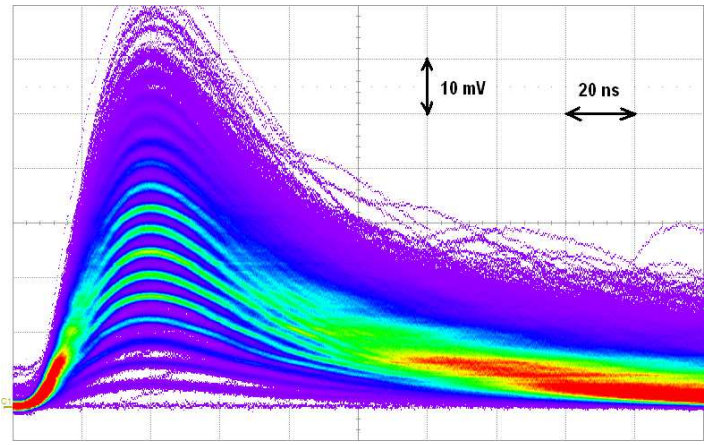

Fig. 2. Superposition of the waveforms of the detected signal on the oscilloscope.

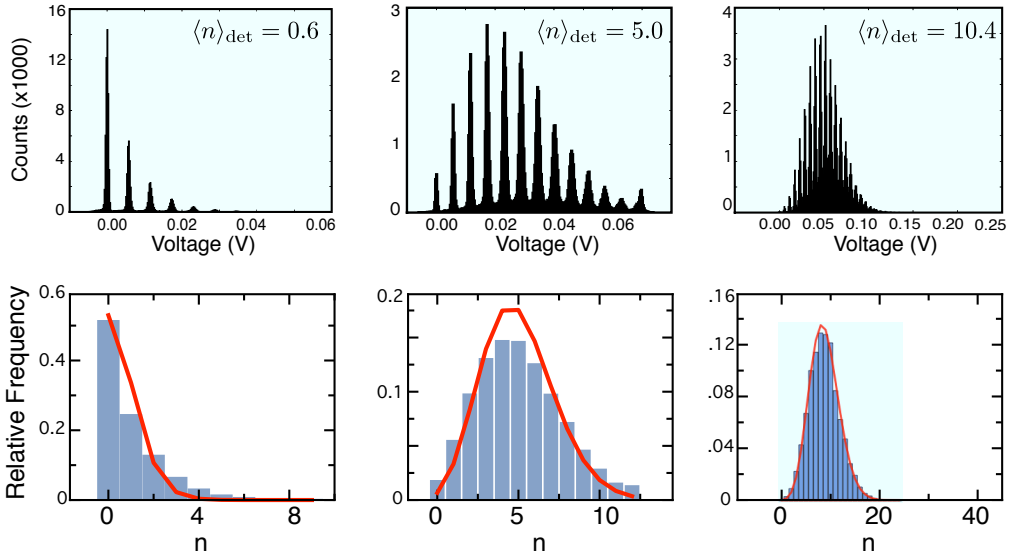

Fig. 3. Top: pulse height histograms for coherent states with mean number simultaneous detections $\langle n \rangle_{det}$ of 0.6, 5.0 and 10.4 respectively. Bottom: corresponding histograms of the relative frequencies of the simultaneous detections, fitted by poissonian distributions (red lines). *n* is the number of simultaneous detections.

0.6, 5.0 and 10.4 respectively. For the first two states one can notice a very good separation between the different amplitude levels. This confirms the good sensitivity of the SiPM and the fact that all the pixels have similar gains. The distinguishability of the peaks gets worse for an increasing number of simultaneous detections, because the uncertainty on the output voltage produced by the firing of N pixels is approximately proportional to $\sqrt{N}$ times the standard deviation of the signal associated to one detection. For the coherent state with $\langle n\rangle_{det}$ =10.4, the peaks are still quite distinct, despite the appearance of a gaussian background due to the overlap of the tails of the detection signals.

For each state the data are organized in a histogram of the relative frequencies of the simultaneous detections, from which we determine the mean ($\langle n\rangle_{det}$) and the variance (σ^2_{det}) values. The data are then fitted with a poissonian distribution, as shown in the three graphs in the lower part of the Figure 3.

2.3. Efficiency and noise characterization

The detector efficiency depends on the efficiency of the whole UC and filtering process and of the SiPM detection efficiency. With the maximum available pump power, the signal at 600 nm measured after the IF is only the 11% of the telecom light sent to the input of the detector, due to the the losses of the system. Only approximately 23% of the telecom light is coupled into the waveguide. A nominal value of 65% should be found for the coupling efficiency at telecom wavelengths. This discrepancy is due to the deterioration in time of the input fiber pigtailing. The number of telecom photons can be upconverted in the PPLN waveguides in principle with a 100% efficiency with a greater pump power [23]. However, the pump power effectively available for the UC is limited by the losses due to fibre splices, to the WDM and also to the waveguide coupling. Finally, the IF has a transmission of 85%.

To analyse the detection system, we send telecom wavelength coherent pulses to the detector with different mean photon numbers $\langle n\rangle_{in}$ at 100 kHz. At this frequency the effects of afterpulsing are negligible, but in principle repetition rates of up to 20 MHz are possible. We measure the efficiency of the SiPM and of the total detector as $\eta = \frac{\langle n\rangle_{det}}{\langle n\rangle_{in}}$, where $\langle n\rangle_{det}$ and $\langle n\rangle_{in}$ are the mean numbers of simultaneous detections and of input photons per pulse, respectively. We measured for the SiPM an efficiency value of η_{SiPM} =36% with the bias voltage at 68.1 V (corresponding to an excess bias voltage of 1.3 V). The excess bias voltage is calculated as the difference between the bias and the breakdown voltage. Notice that the definition of η includes effects of cross-talk, that we will explain in detail in the next paragraph. By counting the total number of detection events, regardless of the amplitude of the avalanches, we can estimate the quantum efficiency of the SiPM to be 24%. The detector is set at a temperature of -34 °C to minimize the thermal noise.

Figure 4 plots the total efficiency η_{tot} of the total detector as a function of $\langle n\rangle_{det}$, for an excess bias voltage of 1.3 V. The detected signal grows linearly with the input signal up to approximately 6 simultaneous detections, and the efficiency of the detector is approximately constant at 4%, which is what we expect from the individual values for the UC and SiPM efficiency. For higher values of $\langle n\rangle_{det}$, η_{tot} decreases because of the saturation of the SiPM. Figure 5 shows the linear trend of the detector efficiency (for low numbers of simultaneous detections) as a function of the excess bias voltage applied to the SiPM. The efficiency shows an increase of (0.31±0.01)% per 0.1 V of excess bias voltage. The amplitude of the avalanches also increases in a linear way with (0.39±0.01)% per 0.1 V of excess bias voltage.

The noise of the detector has two different origins: the electronic noise of the SiPM, which is not produced by incident photons, and the detection of photons at 600 nm originating from other non linear processes (discussed in [24]), which take place inside the waveguide. We calculate the histogram of the detection frequency in the absence of the input telecom signal, from which

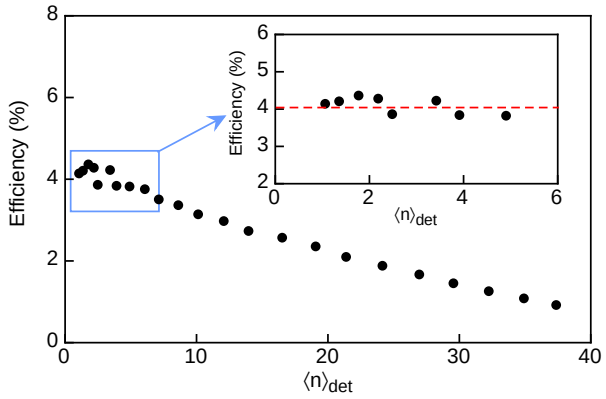

Fig. 4. Efficiency η_{tot} of the UC multi-pixel APD detector as a function of the mean numbers of simultaneous detections $\langle n \rangle_{det}$.

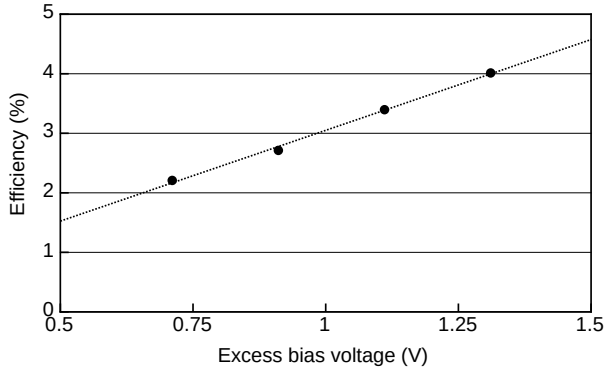

Fig. 5. Efficiency η_{tot} of the UC multi-pixel APD detector as a function of the excess bias voltage applied to the SiPM. The dotted line corresponds to a linear fit of the data.

we find that the noise corresponds to $\langle n \rangle_{det}$=0.023. This value can be interpreted as a noise probability per shot. In order to evaluate the minimal sensitivity of our detector, we divide it by the efficiency of the detector and obtain 0.58. This is the approximate number of incident photons that give the same mean number of detections, if the detector had no noise and if they were sent in pulses of 1 ns width. The majority of this noise is due to the UC. Indeed, only 2% of the total noise is due to the SiPM.

2.4. Multi-photon detection

The multi-photon counting capability of a PNR detector could be in principle characterized by performing a quantum tomography of the detector, according to the method described in [25]. However, in the case of large dynamic range PNR detectors, the number of parameters to find numerically is very large, because probe states with large mean photon numbers have to be used for the characterization of the detector. This makes the numerical problem extremely complex and unstable. Therefore, more practical approaches need to be found for the characterization of PNR detectors in a large photon number regime. In our case we investigate the preservation in

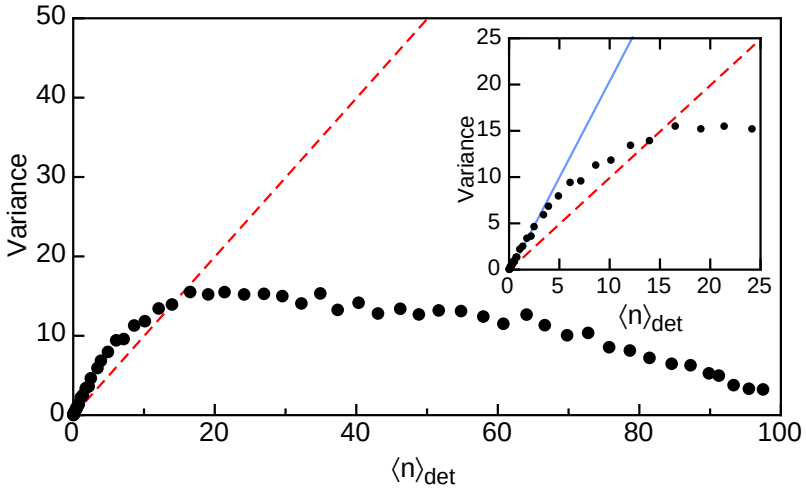

Fig. 6. Experimental variances σ^2_{det} as a function of the corresponding mean numbers of simultaneous detections $\langle n\rangle_{det}$. The dashed red line corresponds to ideally detected coherent states, for which $\sigma^2_{det} = \langle n\rangle_{det}$. In the inset the data for low $\langle n\rangle_{det}$ are shown. The blue line corresponds to the fit of the first data for the calculation of the cross-talk probability of the SiPM.

the detected signal of the statistical properties of the input coherent states. If one sends Fock states to a perfectly efficient PNR detector, with a sufficiently high photon number resolution, distinct outcomes for each state should be expected. In the case of a single shot measurement, one obtains a specific output for only one specific Fock state. For a coherent state a poissonian distribution of outcomes is obtained, thus one can infer the number of photons of the initial pulse only up to the intrinsic uncertainty given by the poissonian statistics.

A good PNR detector should preserve the statistics of the input states: the equality between the mean number of simultaneous detections $\langle n\rangle_{det}$ and the variance of the experimental data distributions σ^2_{det} should be verified. In Figure 6 we plot the experimental variances σ^2_{det} as a function of the corresponding mean numbers of simultaneous detections $\langle n\rangle_{det}$.

The dashed red line in Figure 6 corresponds to the condition of perfect poissonian detection distribution, that is $\langle n\rangle_{det} = \sigma^2_{det}$. The variances of the experimental distributions decrease for more than 20 simultaneous detections due to the saturation of the SiPM. The experimental distributions of the number of simultaneous detections becomes narrower as $\langle n\rangle_{det}$ approaches 100, the number of detector pixels.

The deviation of the experimental variances from the condition of perfectly detected coherent states, for $\langle n\rangle_{det}$ less than 15 (inset of the Figure 6), deserves further discussion. We attribute this fact mainly to optical cross-talk effects between adjacent pixels. The avalanche process in one APD can induce the firing of one ore more neighbouring pixels, as the carriers released during the avalanche can emit radiative photons (the emission probability is approximately one photon per 10^5 carriers) [26]. We determine the cross-talk probability in our detector by considering the recent analytic results reported in [27]. The authors of [27] assume that the pixels can fire because of a primary origin, the detection of a photon, or a secondary one, for cross-talk or afterpulsing, which is essentially random (in our case the afterpulses are negligible.). Because of the latter effect, the experimental distributions of the number of simultaneous detections corresponding to input coherent states are compound poissonians with mean values $\langle n\rangle_{det} = \frac{\langle n\rangle}{1-p}$

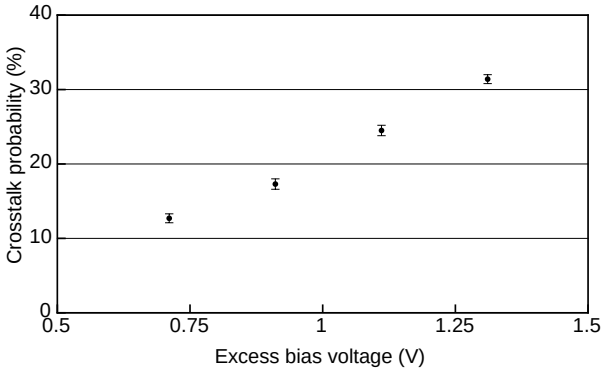

Fig. 7. Cross-talk probability as a function of the excess bias voltage applied to the SiPM. The error bars represent the statistical errors.

and variances $\sigma^2_{det} = \frac{\langle n \rangle (1+p)}{(1-p)^2}$, where p is the probability of firing for secondary events and $\langle n \rangle$ is the mean of the distribution in the absence of cross-talk. According to this model, the mean and the variance of the compound distributions increase in the presence of the secondary effect. The Fano factor F, which is the ratio between the variance of the distribution of the simultaneous detections σ^2_{det} and the mean number of this distribution $\langle n \rangle_{det}$, is thus expressed by the relation $F = \frac{1+p}{1-p}$, from which p can be estimated. We measure F from the slope of the line fitting the data in the inset of Figure 6. We limit the fit to low numbers of $\langle n \rangle_{det}$, where the detector is unaffected by saturation. We obtained a cross-talk probability of $(31.4 \pm 0.6)\%$ at an excess bias voltage of 1.3 V.

The cross-talk probability increases as a function of the excess bias voltage (Figure 7). A similar effect is reported in [28]. The probability for a pixel to fire due to cross-talk is related to its efficiency, but also on the quantity of photons released during the avalanche of a neighbouring pixel, which depends on the amplitude of the avalanches. Both factors increase with the excess bias voltage.

The cross-talk probability affects the values of efficiency η_{SiPM} and η_{tot}. The relation between the value of η and the quantum efficiency of the detector QE can be expressed in our case as $\eta = QE(1+p')$, where p' is the total probability of having detections due to cross-talk of second and multiple order, that is $p' = \sum_{n=1}^{\infty} p^n = \frac{p}{1-p}$, which in our case is $(45.7 \pm 1.3)\%$ at an excess bias voltage of 1.3 V for the value of p determined before. Therefore, we obtain a value of QE_{SiPM}=25% for the SiPM and of QE_{tot}=2.7% for the total detector at an excess bias voltage of 1.3 V. Considering the systematic errors in the estimation of the input photon number, the value of QE_{SiPM} is in good agreement with what we measured directly. Correcting the effects of cross-talk in the detected signal and in the efficiency enables one to perform the calibration of the detector. In other terms it allows one to properly estimate the number of photons in an optical pulse from the detected signal.

3. Conclusion

In this paper we presented a telecom wavelength PNR detector with a large dynamic range, working at room temperature. It is based on the UC of a telecom signal into the visible wavelength regime and detection by a thermoelectrically cooled SiPM. This kind of detector can be used for a wide range of infrared wavelengths with appropriate up-conversion. The efficiency is limited to 4% due to the deteriorated waveguide coupling, however, optimized systems have

achieved pigtailing losses < 0.5dB with further improvements possible [23]. The detector preserves the poissonian statistics of the input coherent states up to 20 simultaneous detections, corresponding to approximately 740 input photons if one considers the quantum efficiency of the detector. The effects of cross-talk in the detected signal can be theoretically estimated. Their correction allows the proper calibration of the detector.

Acknowledgments

This work is supported by the Swiss NCCR "Quantum Photonics". We would like to thank Olivier Guinnard and Claudio Barreiro for their technical support and Patrick Eraerds and Jun Zhang for their valuable comments and suggestions.